Amino Acids (2010) 39:587–597
DOI 10.1007/s00726-010-0480-z

ORIGINAL ARTICLE

# Amphiphilic molecular gels from $\omega$-aminoalkylated L-glutamic acid derivatives with unique chiroptical properties

**Yoshiko Kira · Yutaka Okazaki · Tsuyoshi Sawada · Makoto Takafuji · Hirotaka Ihara**

Received: 2 November 2009 / Accepted: 7 January 2010 / Published online: 27 January 2010


**Abstract** Self-assembling amphiphiles with unique chiroptical properties were derived from L-glutamic acid through $\omega$-aminoalkylation and double long-chain alkylation. These amphiphiles can disperse in various solvents ranging from water to *n*-hexane. TEM and SEM observations indicate that the improvement in dispersity is induced by the formation of tubular and/or fibrillar aggregates with nanosized diameters, which makes these amphiphiles similar to aqueous lipid membrane systems. Spectroscopic observations, such as UV–visible and CD spectroscopies indicate that the aggregates are constructed on the basis of *S*- and *R*-chirally ordered structures through interamide interactions in water and organic media, respectively, and that these chiroptical properties can be controlled thermotropically and lyotropically. It is also reported that the chiral assemblies provide specific binding sites for achiral molecules and then induce chirality for the bonded molecules. Further, the applicability of the amphiphiles to template polymerization is discussed.

**Keywords** Amino acid-derived amphiphilic lipid · Self-assembly · Organic nanotube · Chirally ordered structure · Induced chirality

**Electronic supplementary material** The online version of this article (doi:10.1007/s00726-010-0480-z) contains supplementary material, which is available to authorized users.

Y. Kira · Y. Okazaki · T. Sawada · M. Takafuji · H. Ihara (✉)
Department of Applied Chemistry and Biochemistry,
Kumamoto University, 2-39-1 Kurokami,
Kumamoto 860-8555, Japan
e-mail: ihara@kumamoto-u.ac.jp; ihara@gpo.kumamoto-u.ac.jp

## Introduction

Amino acids are one of the most powerful base materials used for the fabrication of nanoscale organic structures. This is because they are highly versatile biocompatible chemical sources; in addition, the chirality afforded by the asymmetric carbon is essential for the formation of accurate structures with unique functions. A polypeptide, which is a polymer of amino acids, folds into its characteristic three-dimensional structure and behaves as a functional molecule. The formation of regulated conformations of polypeptides, such as $\alpha$-helical and $\beta$-structural polymers, generates secondary chirality, which can be estimated by chiroptical spectroscopies, such as circular dichroism (CD) and optical rotatory dispersion. On the other hand, the chiroptical property based on molecular self-assembly is attracting considerable attention because of the tunability and amplification of chiroptical signals. Therefore, amino acids might potentially find applications in molecular devices, such as sensors and switches (Hembury et al. 2008). In the last two decades, molecular gel systems with chiral low-molecular-weight compounds have been widely investigated. These gels have attracted interest because of the fact that gelation is induced by the formation of a three-dimensional network with nanofibrillar aggregates that are based on highly ordered structures with a unique chirality. Therefore, low-molecular-weight gelators often possess an asymmetric carbon derived from amino acids, sugars, cholesterol, and so on (Terech and Weiss 1997; van Esch and Feringa 2000; Estroff and Hamilton 2004; Ihara et al. 2004; Xue et al. 2004; Shimizu et al. 2005; Oda 2006). The enhancement of the chiroptical properties in molecular gel systems is generally sensitive to external stimuli, such as temperature, light, and electricity. Precise control and accurate detection of the chiroptical property of molecular

gels are important for the development of molecular devices. Thus far, we have focused on L-glutamic acid as a base unit for derivatization into a molecular gelator because of its versatile chemical tunability through its two carboxylic acid groups and one amino group.

In this study, we show that both the dispersity improvement in aqueous and non-aqueous media and the enhancement of chiroptical versatility can be achieved by $\omega$-aminoalkylation into a double long-chain alkylated L-glutamic acid as a self-assembling molecular gelator. Furthermore, we demonstrate that the obtained molecular gels contain nanotubules and nanofibrillar aggregates that provide specific binding sites for achiral guest molecules to induce secondary chirality, and these can be used for template polymerization.

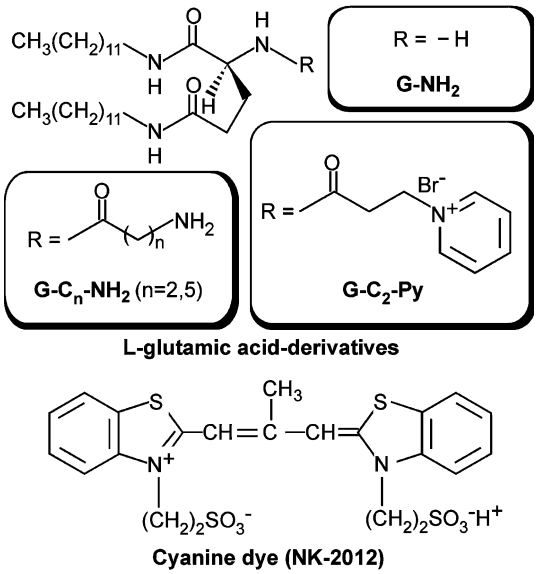


**Scheme 1** Chemical structures of L-glutamic acid-derived amphiphiles and cyanine dye

## Materials and methods

### Chemicals

All chemicals were reagent grade and purchased from chemical suppliers. Tetrahydrofuran (THF) was distilled before use, and all other solvents were used as received. The cyanine dye NK-2012 and the photoinitiator 2-benzyl-2-dimethylamino-1-(4-morpholinophenyl)-butanone-1 (Irgacure 369, $\lambda_{optimal} = 321$ nm) (Timpe et al. 1993; Artal et al. 2001) was used as received. The L-glutamic acid-derived amphiphiles with a $\omega$-amino or an $\omega$-pyridinium head group were synthesized as shown in Scheme 1. The chemical structures of these compounds were identified by melting point, FTIR, $^1$H-NMR and elemental analyses. FTIR spectra were performed using a JASCO FT/IR-4000 spectrometer. $^1$H-NMR spectra were recorded by a JEOL JNM-EX400 spectrometer using tetramethylsilane as an internal standard.

### Preparation of *N*-benzyloxycarbonyl-$\omega$-aminoalkanoic acid

6-Aminohexanoic acid (13.1 g, 100 mmol) was dissolved in 200 ml of a 1 N NaOH, and then benzyloxycarbonyl chloride (21.0 ml, 131 mmol), and 1 N NaOH were added with cooling to 0°C. The mixture was stirred for 1 h at this temperature. After being stirred for 12 h at room temperature, the solution was washed with diethyl ether. Then, 1 N HCl was added into the water phase until the pH became 1. The solution separated into water and oil phases. The oil phase was extracted by washing with ethyl acetate. The ethyl acetate phase was dried over $Na_2SO_4$, concentrated in vacuo. The residue was recrystallized from *n*-hexane and dried in vacuo to yield a white solid powder. Yield: 21.9 g (88%). mp: 54–56°C. IR (KBr): 3,344, 1,688, 1,545 cm$^{-1}$. $^1$H-NMR ($CDCl_3$, 400 MHz): $\delta$ 1.37 [tt, J 7.3, 7.3 Hz, 2H, C$H_2$(CH$_2$)$_2$NH], 1.53 (tt, J 7.3, 7.3 Hz, 2H, C$H_2$CH$_2$NH), 1.65 (tt, J 7.3, 7.3 Hz, 2H, HO$_2$CCH$_2$C$H_2$), 2.35 (t, J 7.3 Hz, 2H, HO$_2$CC$H_2$), 3.20 (dt, J 7.3, 7.3 Hz, 2H, C$H_2$NH), 4.77 (br s, 1H, N*H*), 5.09 (br s, 2H, C$H_2$Ph), 7.31–7.36 (m, 5H, aromatics).

*N*-Benzyloxycarbonyl-3-aminopropionic acid was prepared using 3-aminopropionic acid according to the similar procedure. mp: 105–106°C. IR (KBr): 3,335, 1,685, 1,536 cm$^{-1}$. $^1$H-NMR ($CDCl_3$, 400 MHz): $\delta$ 2.61 (t, J 5.9 Hz, 2H, HO$_2$CC$H_2$), 3.47 (dt, J 5.9, 5.9 Hz, 1H, C$H_2$NH), 5.10 (br s, 2H, C$H_2$Ph), 5.29 (br s, 1H, N*H*), 7.24–7.40 (m, 5H, aromatics).

### Preparation of L-glutaminic acid didodecylamide (G–NH$_2$)

*N*-Benzyloxycarbonyl-L-glutamic acid didodecylamide (G–Z, Gopal et al. 2006) was prepared by a coupling reaction of *N*-benzyloxycarbonyl-L-glutamic acid with dodecylamine in THF using diethylphosphorocyanidate (DEPC), and then L-glutaminic acid didodecylamide (G–NH$_2$, Gopal et al. 2006) was prepared by debenzyloxycarbonylation of G–Z in 200 ml of ethanol with H$_2$/Pd–carbon according to the previously reported procedure.

### Preparation of *N*-(benzyloxycarbonyl-$\omega$-aminoalkanoyl)-L-glutamic acid didodecylamide (G–C$_n$–Z)

*N*-(Benzyloxycarbonyl-6-aminohexanoyl)-L-glutamic acid didodecylamide (G–C$_5$–Z) was prepared by following

procedure. G–$NH_2$ (4.3 g, 8.9 mmol), *N*-benzyloxycarbonyl-6-aminohexanoic acid (3.1 g, 11.7 mmol), and triethylamine (2.5 ml, 18.0 mmol) were dissolved in THF (350 ml). The solution was cooled to 0°C, and DEPC (2.0 ml, 13.2 mmol) was added to the solution. The mixture was stirred for 1 h at this temperature. After being stirred for 12 h at room temperature, the solution was concentrated in vacuo, and the residue was dissolved in chloroform. The solution was washed with 0.2 N NaOH, 0.2 N HCl, and water. The solution was dried over $Na_2SO_4$, concentrated in vacuo and the residue was dissolved in *N*,*N*-dimethylformamide. Then, this solution was put into water and white crystals appeared and were corrected by filtration. Yield: 5.20 g (88%). mp: 159–160°C. IR (KBr): 3,295, 2,920, 2,851, 1,687, 1,635, 1,548 $cm^{-1}$. $^1$H-NMR: $\delta$ 0.88 (t, J 6.8 Hz, 6H, C$H_3$), 1.25 [br s, 36H, $CH_3(CH_2)_9$], 1.42–1.56 (m, 6H, $CH_2(CH_2)_3CH_2NHCO$), 1.56–1.72 (m, 4H, $CH_2CH_2NHCO$), 1.85–2.11 (m, 2H, C*HC$H_2$), 2.22 (t, J 7.3 Hz, 2H, NHCOC$H_2CH_2(CH_2)_4N$), 2.16–2.54 (m, 2H, NHCOC$H_2CH_2$C*), 3.19 (dt, J 7.3, 7.3 Hz, 2H, C$H_2$NHCO), 3.23 (dt, J 7.3, 7.3 Hz, 4H, C$H_2$NHCO), 4.31 (dt, J 7.3, 4.9 Hz, 1H, C*$H$), 4.86 (br s, 1H, N$H$), 5.10 (br s, 2H, C$H_2$Ph), 6.01 (br s, 1H, N$H$), 6.80 (br s, 1H, N$H$), 7.28–7.42 (m, 5H, aromatics). Anal. calcd for $C_{43}H_{76}N_4O_5$: C, 70.8; H, 10.5; N, 7.68. Found: C, 69.8; H, 10.3; N, 7.68.

Preparation of *N*-(benzyloxycarbonyl-3-aminopropanoyl)-L-glutamic acid didodecylamide (G–$C_2$–Z) was prepared from a coupling reaction of G–$NH_2$ with *N*-benzyloxycarbonyl-3-aminopropionic acid according to the similar synthetic procedure of G–$C_5$–Z. After recrystallization from ethanol, white powders were obtained. mp: 174–175°C. IR (KBr): 3,295, 2,921, 2,851, 1,698, 1,637, 1,550 $cm^{-1}$. $^1$H-NMR ($CDCl_3$) $\delta$ 0.88 [t, J 7.3 Hz, 6H, C$H_3$), 1.26 (br s, 36H, $CH_3(CH_2)_9$], 1.49 (tt, J 7.3, 7.3 Hz, 4H, C$H_2CH_2NHCO$), 1.86–2.10 (m, 2H, C*HC$H_2$), 2.46 (t, J 5.8 Hz, 2H, NHCOC$H_2CH_2$N), 2.19–2.52 (m, 2H, NHCOC$H_2CH_2$C*), 3.23 (dt, J 5.8, 6.8 Hz, 2H, C$H_2$NHCO), 3.40–3.56 (br m, NHCOC$H_2CH_2$N), 4.33 (dt, J 5.8, 6.8 Hz, 1H, C*$H$), 5.14 (br s, 2H, C$H_2$Ph), 5.09 (br s, 1H, N$H$), 5.82 (br s, 1H, N$H$), 6.82 (br s, 1H, N$H$), 7.13 (br s, 1H, N$H$), 7.29–7.45 (m, 5H, aromatics). Anal. calcd for $C_{40}H_{70}N_4O_5$: C, 70.1; H, 10.3; N, 8.08. Found: H, 10.3; C, 69.9; N, 8.15.

## Preparation of ω-aminoalkanoyl-L-glutamic acid didodecylamide (G–$C_n$–$NH_2$)

6-Aminohexanoyl-L-glutamic acid didodecylamide (G–$C_5$–$NH_2$) was prepared by following procedure. G–$C_5$–Z (3.0 g, 4.1 mmol) was dissolved in 200 ml of ethanol at 60°C, and Pd–carbon (0.6 g) was added to the solution. After $H_2$ gas was bubbled slowly into the solution for 8 h at 70°C, Pd–carbon was removed by filtration. The solution was concentrated in vacuo and the residue was dissolved in chloroform. Then, this solution was put into acetonitrile and white crystals appeared and were corrected by filtration. Yield: 2.0 g (82%). mp: 128–130°C. IR (KBr) 3,289, 2,919, 2,851, 1,636, 1,558, 1,542 $cm^{-1}$. $^1$H-NMR ($CDCl_3$, 400 MHz) $\delta$ 0.88 (t, J 6.8 Hz, 6H, C$H_3$), 1.25 [br s, 36H, $CH_3(CH_2)_9$], 1.41–1.57 [m, 6H, $CH_2(CH_2)_3CH_2NH_2$], 1.66 (tt, J 7.3, 7.3 Hz, 4H, C$H_2CH_2NHCO$), 1.85–2.15 (m, 2H, C*HC$H_2$), 2.24 [t, J 7.8 Hz, 2H, NHCOC$H_2(CH_2)_4NH_2$], 2.16–2.54 (m, 4H, NHCOC$H_2$ $CH_2$C*), 2.69 (t, J 6.8 Hz, 2H, C$H_2NH_2$), 3.23 (dt, J 6.8, 6.8 Hz, 4H, C$H_2$NHCO), 4.33 (dt, 5.9, 6.8 Hz, 1H, C*$H$), 6.07 (br s, 1H, N$H$), 6.82 (br s, 1H, N$H$), 7.26 (br s, 1H, N$H$). Anal. calcd for $C_{35}H_{70}N_4O_3$: C, 70.1; H, 11.9; N, 9.42%. Found: H, 11.3; C, 68.7; N, 8.67.

3-Aminopropanoyl-L-glutamic acid didodecylamide (G–$C_2$–$NH_2$) was also prepared from G–$C_2$–Z according to the similar synthetic procedure of G–$C_5$–$NH_2$. After recrystallization from ethanol, white powders were obtained. mp: 136–138°C. IR (KBr): 3,292, 2,920, 2,851, 1,638, 1,555 $cm^{-1}$. $^1$H-NMR ($CDCl_3$, 400 MHz) $\delta$ 0.89 (t, J 6.8 Hz, 6H, C$H_3$), 1.26 (br s, 36H, $CH_3(CH_2)_9$), 1.48 (br s, 4H, C$H_2CH_2NHCO$), 1.91–2.17 (m, 2H, C*HC$H_2$), 2.23–2.48 (m, 2H, NHCOC$H_2$), 2.36 (t, J 6.3 Hz, 2H, NHCOC$H_2CH_2NH_2$), 3.04 (t, J 6.3 Hz, 2H, C$H_2NH_2$), 3.22 (dt, J 6.8, 6.8 Hz, 4H, C$H_2$NHCO), 4.38 (dt, J 6.3, 7.8 Hz, 1H, C*$H$), 6.02 (br s, 1H, N$H$), 7.09 (br s, 1H, N$H$), 7.93 (br s, 1H, N$H$). Anal. calcd for $C_{32}H_{64}N_4O_3$: C, 69.6; H, 11.6; N, 10.2%. Found: C, 68.0; H, 11.3; N, 9.45.

## Preparation of *N*-(3-pyridinium propionyl)-L-glutamic acid didodecylamide bromide (G–$C_2$–Py)

3-Bromopropionyl-L-glutamic acid didodecylamide (G–$C_2$–Br, Gopal et al. 2006) was prepared by a coupling reaction of G–$NH_2$ with 3-bromopropionic acid, and then *N*-(3-pyridinium propionyl)-L-glutamic acid didodecylamide bromide (G–$C_2$–Py, Gopal et al. 2006) was prepared by quaternization of pyridine with G–$C_2$–Br according to the previously reported procedure.

## Polymerization of styrene in G–$C_2$–Py

G–$C_2$–Py (10 mg, 14.3 mmol) was dissolved in 2.5-ml water and vortexed for 1 min at room temperature. The solution was sonicated using a SONICATOR XL2020 (Misonix Inc.) equipped with a Ti microprobe tip ($\phi$ 1.6 mm, 20 W) for 5 min at about 60°C and allowed to stand for 30 min at room temperature. Methanol (0.1 ml) containing Irgacure 369 (0.5 mg) and styrene (10 mg) were added into the G–$C_2$–Py aqueous solution and vortexed for 1 min at room temperature. The mixture was diluted by water to become the concentration of G–$C_2$–Py to 0.5 mM

and furthermore vortexed for 1 min at room temperature. Remaining oxygen was removed by bubbling a nitrogen gas. The solution was replaced into a 1-mm quarts cell, aged at 10°C for 1 h and irradiated by UV light ranging of 280–370 nm with the IR cut filter and UV transmittance filter. Photo-induced polymerization was carried out using OPM-×500 (ultrahigh-pressure mercury lamp of 0.75 kW power) from Ushio Inc. and spectroscopically monitored by the absorption decrease at 247 nm.

### Measurements

Transmission electron microscope (TEM) images were recorded using a JEOL JEM-2000FX. The samples were spotted on polyvinyl-formal-coated copper grids. Following the excess of the samples was removed by a tissue paper and the samples were air-dried, the samples were stained with a 1 wt% uranyl acetate aqueous solution. Scanning electron microscope (SEM) images of the xerogels were recorded using a JEOL JCM-5700. The critical gelation concentration (CGC) was determined by an inversion fluid method using an $\phi$ 10-mm test tube (Ihara et al. 2002). The xerogel was prepared from organogel using freeze drying, and osmium was coated onto the xerogel using Filgen Osmium Plasma Coater OPC60A. UV–visible and CD spectra were recorded using JASCO V-560 and JASCO J-725 spectrometers, respectively, and the temperature was controlled by a Peltier thermostated cell holder. Differential scanning calorimetry (DSC) analysis of the L-glutamic acid-derived amphiphiles was carried out using DSC6200 and EXTRA 6000 from Seiko Instruments Inc. The aqueous solution of these amphiphiles (20 mM, 50 µl) was sealed in 70-µl silver pan and measured between 10 and 80°C at heating and cooling rate of 2°C/min.

## Results and discussion

### Unique dispersity of $\omega$-aminoalkyloyl L-glutamic acid amphiphiles

The improvement of the dispersity of molecular tools in solvents expands the possible applicability of amphiphiles. The dispersity of L-glutamic acid-derived amphiphiles was examined in various solvents ranging from water to *n*-hexane. As summarized in Table 1, the dispersity of the double long-chain alkylated L-glutamic acid (G–$NH_2$) was remarkably improved by $\omega$-aminoalkylation when compared with that of G–$C_2$–$NH_2$ and G–$C_5$–$NH_2$, as shown in Scheme 2.

TEM observation indicates that the enhanced dispersity can be explained by the formation of fibrillar aggregates in both water and organic media. Figures 1 and 2 show the typical aggregation morphologies of these fibrils. It is clearly observed that G–$C_2$–$NH_2$ and G–$C_5$–$NH_2$ form tubules and/or fibrils with nanosized diameters (outer diameter 15–25 nm) in water and organic media, such as acetonitrile, benzene, and cyclohexane, whereas G–$NH_2$ without $\omega$-aminoalkylation forms only globular aggregates, such as vesicles in water (Fig. 1a). However, no results with organic solvents have been obtained thus far because of the poor solubility of the samples in these solvents.

**Table 1** Dispersity of L-glutamic acid-derived amphiphiles in various solvents

| | G–$NH_2$ | G–$C_2$–Py | G–$C_2$–$NH_2$ | G–$C_5$–$NH_2$ |
|---|---|---|---|---|
| Water | S | S | S | S |
| Methanol | S | S | S | S |
| Ethanol | S | S | S | S |
| Acetonitrile | I | S | S | S |
| *N,N*-Dimethylformamide | S | S | S | S |
| Chloroform | S | S | S | S |
| Tetrahydrofuran | S | I | S | S |
| Acetone | S | I | S | S |
| Ethylacetate | I | I | S | S |
| Benzene | S | S | S | S |
| Toluene | S | S | S | S |
| Cyclohexane | I | I | S | S |
| Diethyl ether | I | I | S | S |
| *n*-Hexane | I | I | S | S |

*S* and *I* indicate to be a clear solution and hard to solve in 1 mM at 10°C, respectively

G–$C_2$–$NH_2$ and G–$C_5$–$NH_2$ exhibit gelation ability with an increase in concentration, as shown in Fig. 3. This is distinctly observed in organic media because the increase in concentration promotes the development of fibrillar structures into a three-dimensional network. This can be confirmed by the SEM observation of the xerogels prepared by freeze drying the organogel. Figure 3 shows a typical example of the G–$C_2$–$NH_2$ benzene gel and its SEM image. From the SEM image, the diameters of the fibrils are observed to be 100–500 nm; these values are considerably larger than the values of 15–25 nm obtained from TEM observations. This is probably attributable to bundle formation during the drying process.

Gels in an organic medium exhibit a CGC. These concentrations are evaluated by using a conventional inversion method. In the case of G–$C_2$–$NH_2$, a sol to gel transformation is observed in the concentration range of 0.1–0.5, 0.5–1.0, and 0.5–1.0 mM at 10°C in acetonitrile, benzene, and cyclohexane, respectively. These phenomena are known as low-molecular-mass gelation in organic media (Terech and Weiss 1997; van Esch and Feringa 2000; Ihara et al. 2004; Oda 2006; Simalou et al. 2009). Similarity of

**Scheme 2** Synthetic procedure of L-glutamic acid-derived amphiphiles

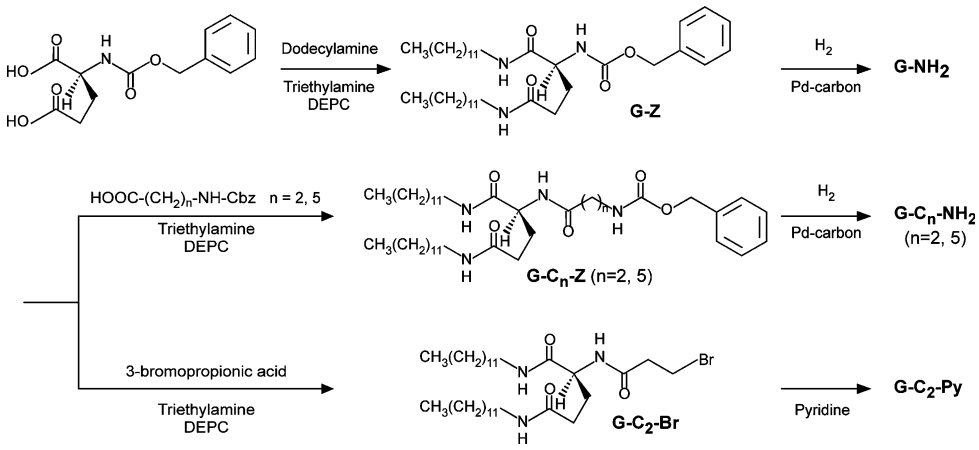


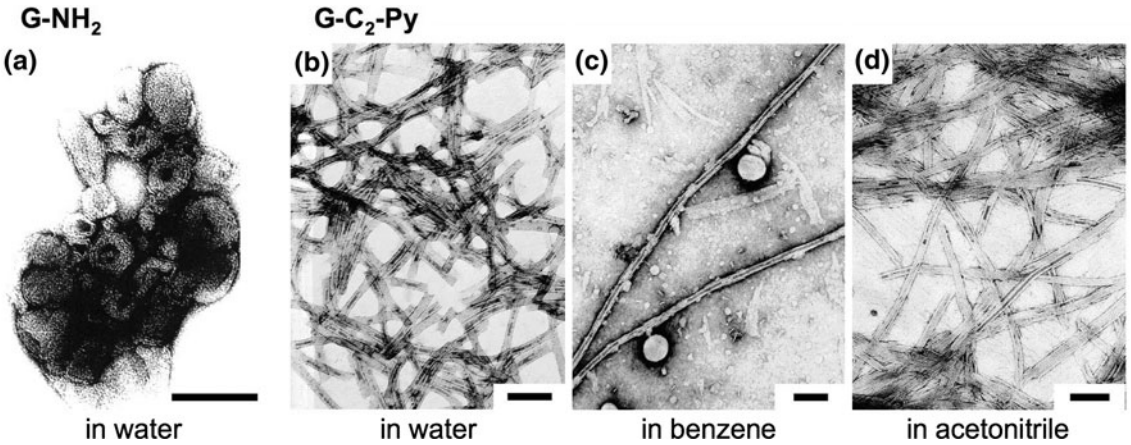


**Fig. 1** TEM images of G–$NH_2$ (**a**) and G–$C_2$–Py (**b**–**d**) aggregates in various solvents. Initial concentration: 0.2–0.5 mM. *Scale bars* 100 nm

gelation property is obtained in G–$C_5$–$NH_2$, but not in G–$C_2$–Py. Table 2 summarizes the CGC of G–$C_2$–$NH_2$ and G–$C_5$–$NH_2$ in various solvents at 10°C.

On the other hand, G–$C_2$–$NH_2$ and G–$C_5$–$NH_2$ do not exhibit a distinct CGC in water even at a high concentration, such as 20 mM, although the viscosity increases remarkably. In addition, the viscosity of G–$C_5$–$NH_2$ is higher than that of G–$C_2$–$NH_2$. This is related to the fact that G–$C_2$–$NH_2$ can mainly form short tubules in water, whereas G–$C_5$–$NH_2$ can form developed, twisted, ribbon-like aggregates (Fig. 2).

## Formation of nanotubular structures in both aqueous and non-aqueous media

G–$C_2$–Py is a derivative of G–$NH_2$ with a pyridinium head group. The dispersity of G–$C_2$–Py in organic solvents is not improved because of its ionic property; however, the aggregation behavior changes significantly. This suggests that the alkyl spacer chain between a L-glutamic acid moiety and a hydrophilic group promotes the transformation of the aggregation morphology to a fibrillar form. Interestingly, as shown in Fig. 1c and d, nanotubular structures are produced even in organic media, such as acetonitrile and benzene. The thicknesses of these aggregates are ca. 5–6 nm, indicating the bimolecular length of G–$C_2$–Py. Therefore, it can be concluded that the tubular structures are based on bilayered structures similar to aqueous lipid bilayered membranes (Kim and Needham 2002). It is known that organogel-forming low-molecular-weight compounds can form nanofibrillar aggregates; however, G–$C_2$–Py is the first example that can produce bilayer-based nanotubular aggregates in both aqueous and non-aqueous organic media.

## Chiroptical property in aqueous system

In aqueous media, G–$C_2$–$NH_2$ provides negative and strong Cotton effects ($[\theta]_{max}$ = ca. $-1.0 \times 10^5$ deg cm$^2$ d mol$^{-1}$ at 10°C) in the absorption band around 200 nm, which is assigned to the amide bonds (Fig. 4c). This CD intensity is almost 20 times larger than that in the molecular-based chirality of G–$C_2$–$NH_2$. On the other hand, the temperature-$[\theta]_{max}$ plots of Fig. 4d show that the CD strength is

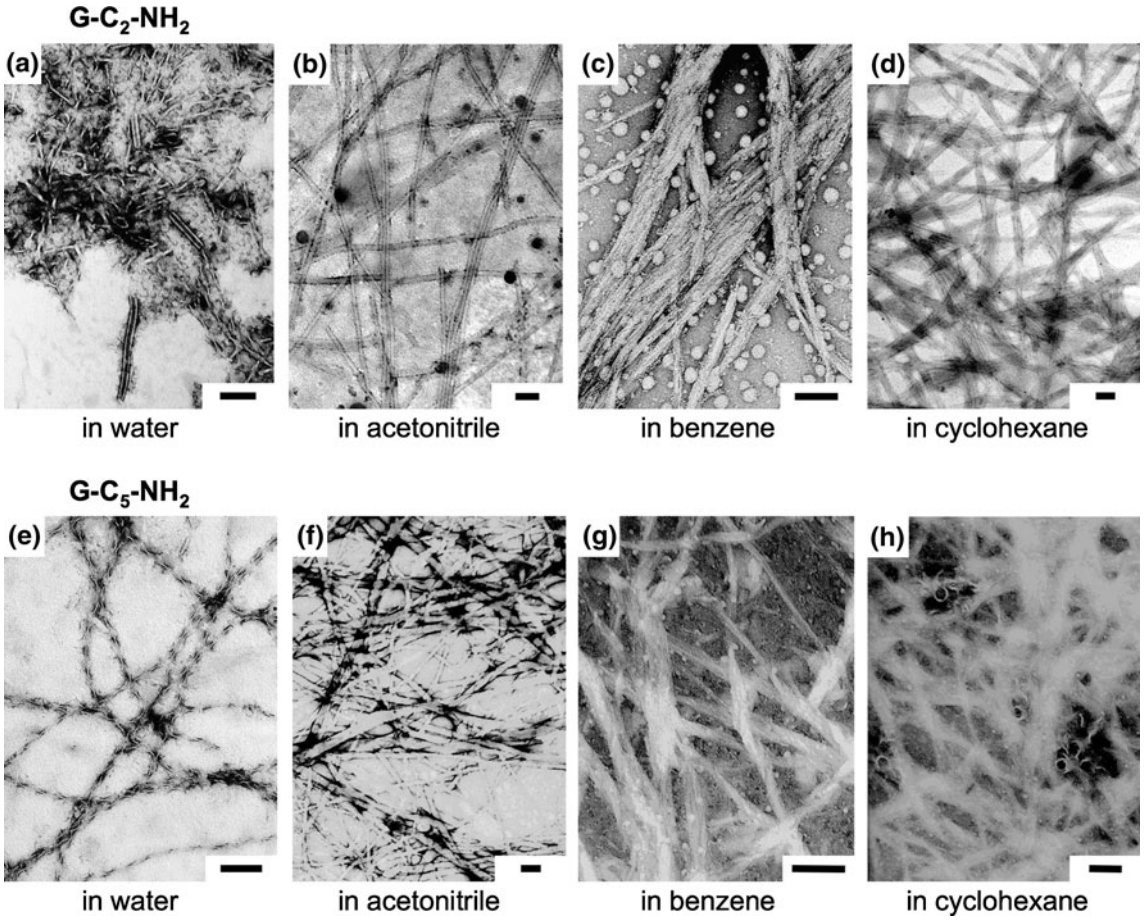


**Fig. 2** TEM images of G–$C_2$–$NH_2$ (**a**–**d**) and G–$C_5$–$NH_2$ (**e**–**h**) aggregates in various solvents. Initial concentration: 0.05–0.5 mM. *Scale bars* 100 nm

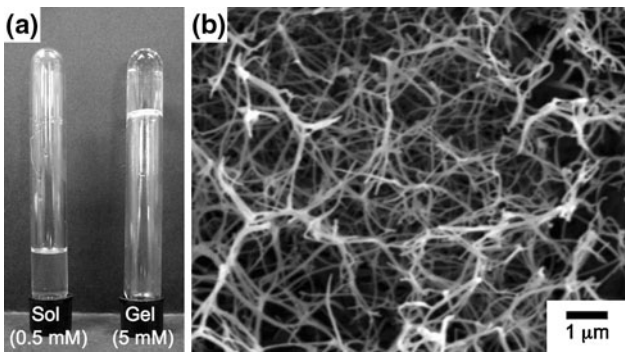


**Fig. 3** **a** Typical example of the concentration-dependent gel to sol transformation of G–$C_2$–$NH_2$ in benzene. The gel–sol transition is observed in the concentration ranging in 0.5–1.0 mM in benzene at 10°C. **b** SEM image of a xelogel prepared from freeze drying of a G–$C_2$–$NH_2$ benzene gel (20 mM)

remarkably temperature dependent and strongly suggest that the critical temperature lies in the temperature range around 35–40°C.

The thermotropic phase transition behavior of G–$C_2$–$NH_2$ in water can also be detected by DSC at a high concentration (20 mM). The observed DSC thermogram exhibits an endothermic curve with a peak at 37°C and a shoulder at 30°C (Fig. 4b) and an exothermic curve, with a

**Table 2** Critical gelation concentration of L-glutamic acid-derived amphiphiles in various solvents at 10°C

| | G–$C_2$–Py | G–$C_2$–$NH_2$ | G–$C_5$–$NH_2$ |
|---|---|---|---|
| Water | >20 mM | >20 mM | >20 mM |
| Methanol | >20 mM | >20 mM | 7.5–10 mM |
| Ethanol | >20 mM | >20 mM | 10–20 mM |
| Acetonitrile | >20 mM | 0.1–0.5 mM | 1.0–2.5 mM |
| *N,N*-Dimethylformamide | >20 mM | >20 mM | 1.0–2.5 mM |
| Chloroform | >20 mM | >20 mM | >20 mM |
| Tetrahydrofuran | – | 7.5–10 mM | 2.5–5.0 mM |
| Acetone | – | 2.5–5.0 mM | 2.5–5.0 mM |
| Ethylacetate | – | 1.0–2.5 mM | 1.0–2.5 mM |
| Benzene | >20 mM | 0.5–1.0 mM | 1.0–2.5 mM |
| Toluene | 10–20 mM | 0.5–1.0 mM | 1.0–2.5 mM |
| Cyclohexane | – | 0.5–1.0 mM | 1.0–2.5 mM |
| Diethyl ether | – | 0.5–1.0 mM | 1.0–2.5 mM |
| *n*-Hexane | – | 0.1–0.5 mM | 0.5–1.0 mM |

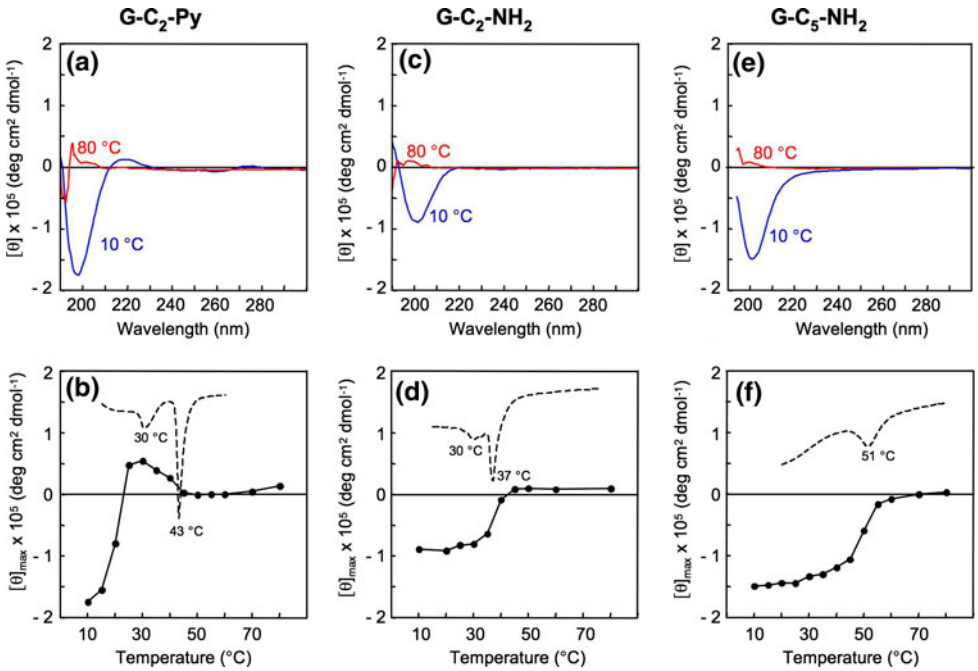


**Fig. 4** CD spectra (**a**, **c**, **e**) and temperature-$[\theta]_{max}$ plots (**b**, **d**, **f**) of G–$C_2$–Py, G–$C_2$–$NH_2$ and G–$C_5$–$NH_2$ in water (0.5 mM). The *dotted lines* indicate DSC thermograms obtained in the heating process in water (20 mM)

peak at 18°C in the heating and cooling process, respectively. Because these phenomena are thermally reversible, it is confirmed that the G–$C_2$–$NH_2$ assembly exhibits thermotropic phase transition in water. This observation is similar to the behavior of the gel to liquid crystalline phase transition of lipid membranes in an aqueous solution (Matsui and Kaneshima 2002). Therefore, the enhanced CD intensity at a low temperature is attributed to the induction of the secondary chirality with *S*-chiral stacking (Simonyi et al. 2003) based on highly ordered aggregation.

Similar chiroptical properties with thermotropic phase transitions are also observed in G–$C_2$–Py and G–$C_5$–$NH_2$, as shown in Fig. 4a, b, e, and f, whereas G–$C_2$–Py exhibits a specific temperature dependence around 25–45°C.

## Chiroptical property in non-aqueous system

G–$C_2$–$NH_2$ and G–$C_5$–$NH_2$ in acetonitrile exhibit a positive cotton effect in the absorption band around 200 nm that is several times stronger than that in water (Fig. 5a, b). A similar positive cotton effect with a small negative band at 220 nm was observed in cyclohexane (Fig. 5c, d). These results indicate that *R* chirally (Simonyi et al. 2003) ordered structures are mainly produced in organic solvents through interamide bonding interactions, and the detailed ordering state is dependent on the type of solvent used, whereas *S*-chiral ordering is dominant in water.

Figure 5 shows the temperature dependence of CD spectra. As in the case of water, the CD intensity decreases with an increase in the temperature; however, there is no distinct critical temperature. This observation is supported by the fact that the DSC does not indicate any phase transition behavior at temperatures between 10 and 80°C. TEM observation shows that only fragmented fibrils can be found at a high temperature.

## Host–guest function as chiral assembly

It is known that chiral assemblies with highly ordered structures often provide specific binding sites for achiral

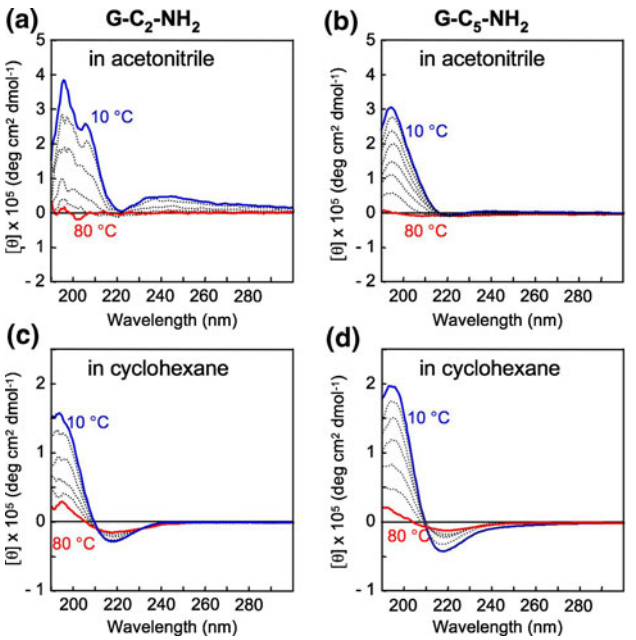


**Fig. 5** Temperature dependencies of CD spectra of G–$C_2$–$NH_2$ (**a**, **c**) and G–$C_5$–$NH_5$ (**b**, **d**) in acetonitrile (0.2 mM) and cyclohexane (0.5 mM)

molecules and then induce secondary chirality for the bonded molecules (Hatano et al 1973; Nakashima et al. 1981; Shibata et al. 1993). Therefore, this phenomenon can be useful as an informative evaluation method for L-glutamic acid-based chiral assemblies. Figure 6 shows UV–visible and CD spectra in the mixed system with a cyanine dye NK-2012 as an anionic achiral molecule in water. $\lambda_{max}$ in NK-2012 appeared at 543 nm in aqueous solution and shifted to 507 and 503 nm in the G–$C_2$–Py and G–$C_2$–$NH_2$ systems, respectively. These typical blue shifts are accompanied by the induction of large cotton effects (Fig. 6b, d). These spectral patterns indicate that almost all the NK-2012 combines with the G–$C_2$–Py and G–$C_2$–$NH_2$ assemblies, probably due to electrostatic interaction, and this host–guest system promotes an *H*-like aggregation of the NK-2012 as a head-to-head stacking state (Shibata et al. 1993; Mishra et al. 2000; Sagawa et al. 2004). In addition, the CD patterns support the speculation that the aggregation is based on *S*-chiral ordering. In contrast, the NK-2012 in the G–$C_5$–$NH_2$ system exhibits two absorption bands from $\lambda_{max}$ of 543 nm: one is a blue-shifted band at $\lambda_{max}$ of 501 nm due to *H*-like aggregation and the other is a red-shifted band at $\lambda_{max}$ of 576 nm due to *J*-like aggregation (Fig. 6e). Interestingly, these $\lambda_{max}$ shifts are accompanied by inductions of *S*-chirality and *R*-chirality, respectively (Fig. 6f). Therefore, the G–$C_5$–$NH_2$ assembly posses two types of chirally specific binding sites that are based on the $C_5$ moiety.

The binding behavior of NK-2012 in an organic medium is also examined by using a cyclohexane–ethanol mixture (20:1) because of the limitation of the solubility for NK-2012. The sample mixtures are prepared by mixing an ethanol solution of NK-2012 (0.2 mM, 200 µl) with a cyclohexane solution of L-glutamic acid-derived amphiphiles (0.5 mM, 4 ml) at 10°C. As shown in Fig. 7, the induction of CD signals is observed around $\lambda_{max}$ (429 nm) of NK-2012 in the G–$C_2$–$NH_2$ system at 10°C. These results indicate that the G–$C_2$–$NH_2$ assembly can provide chirally specific binding sites even in an organic medium. NK-2012 probably forms *H*-like aggregates with *R*-chiral arrangement in the G–$C_2$–$NH_2$ system. The solubility of the dye-G–$C_2$–$NH_2$ assembly complex decreases above 55°C and precipitation is confirmed at 70°C. In this case, an amino group of G–$C_2$–$NH_2$ does not form ammonium ions. Therefore, it is considered that the NK-2012 binds to the G–$C_2$–NH2 assembly thorough polar interaction. In contrast, almost no CD induction is detected around $\lambda_{max}$ of NK-2012 in the G–$C_5$–$NH_2$ system regardless of the existence of the *H*-like aggregate species that produces $\lambda_{max}$ around 450 nm at 10°C. These results are probably explained by the non-chirally stacked binding of NK-2012 on the G–$C_5$–$NH_2$ assembly. In this case, the $C_5$ spacer chain can become rather flexible by solvation, resulting in the disordering of the $NH_2$ moiety even if the L-glutamic acid moiety is in an ordered state through an interamide interaction. In the case of a dye-G–$C_5$–$NH_2$ assembly complex, no precipitation is observed even at 70°C; however, monomeric species with $\lambda_{max}$ of 563 nm increase with temperature. This is probably due to the disordered state of G–$C_5$–$NH_2$ molecules at higher temperatures. Figure 8 shows schematic representations of the binding behaviors of NK-2012 on and/or in the chiral assemblies in aqueous and non-aqueous systems.

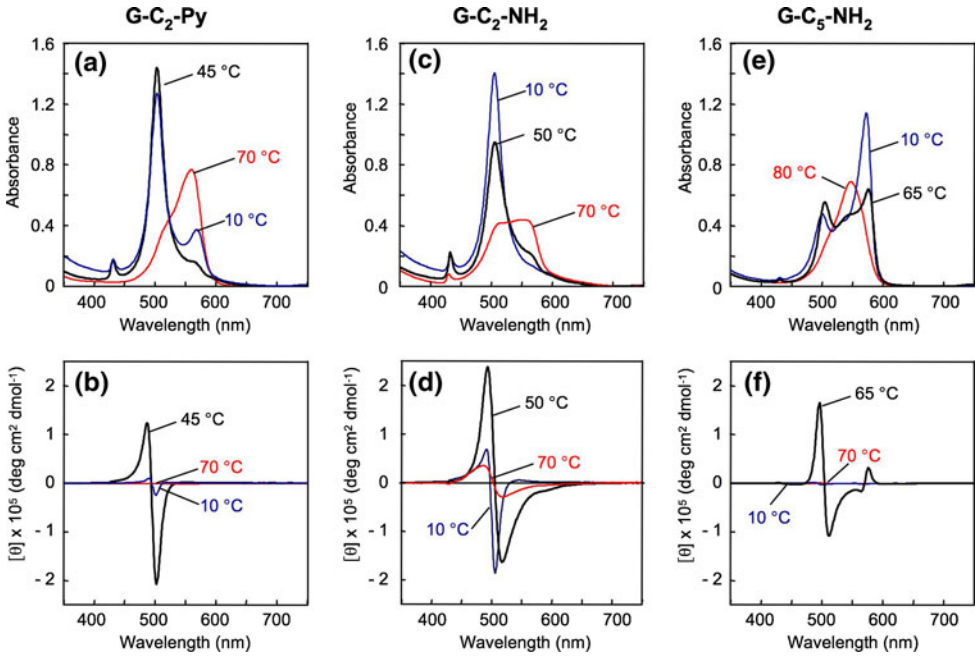


**Fig. 6** UV–visible and CD spectra of NK-2012 (0.01 mM) in the presence of G–$C_2$–Py, G–$C_2$–$NH_2$ and G–$C_5$–$NH_2$ (0.5 mM) in water

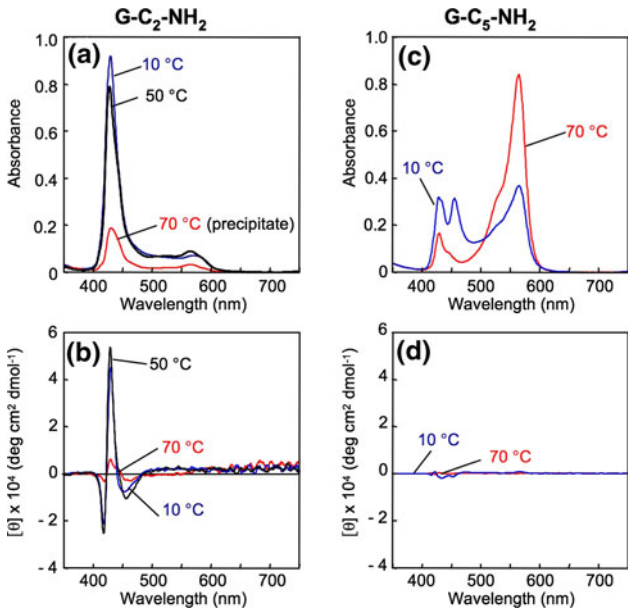


**Fig. 7** UV–visible and CD spectra of NK-2012 (0.01 mM) in the presence of G–$C_2$–$NH_2$ and G–$C_5$–$NH_2$ (0.5 mM) in a cyclohexane–ethanol mixture (20:1)

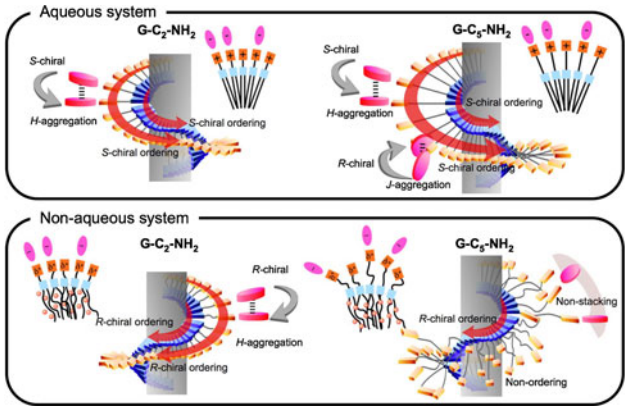


**Fig. 8** Schematic illustration of the binding behaviors of NK-2012 on and/or in the chiral assemblies in aqueous and non-aqueous systems

## Host–guest function for template polymerization

Nanostructures based on bilayer membranes such as vesicles and rods are expected to function as a specific medium for the preparation of nanostructures by polymerization (Hotz and Meier 1998; Becerra et al. 2004; da Silva Gomes et al. 2006; Dergunov and Pinkhassik 2008). Tekobo and Pinkhassik (2009) used nanodisks prepared by a phospholipids for the polymerization of styrene and reported that disk-like polymers could be produced. In this work, photo-induced radical polymerization of styrene is investigated in the presence of aqueous G–$C_2$–Py nanotubes.

The mixed samples of styrene with G–$C_2$–Py are prepared by injecting a given amount of styrene into an aqueous G–$C_2$–Py solution and ultrasonicating the sample. The resultant mixtures are almost clear to slightly turbid depending on the amount of styrene. Figure 9a shows a TEM image of G–$C_2$–Py before the addition of styrene. It is found that the main products are nanotubes with outer diameters of 15–17 nm and a length of ca. 100–500 nm. The membrane thickness is 5–6 nm, which corresponds to the bimolecular length of G–$C_2$–Py. As shown in Fig. 9b, the addition of styrene induces significant changes in the aggregation morphology. For example, by the addition of an equal amount of styrene to G–$C_2$–Py, the outer diameter and membrane thickness were found to increase from 18 to 22 and 7 to 9 nm, respectively. A further distinct change is a one-dimensional one in that the length increases to more than 1,000 nm. Therefore, it is proved that G–$C_2$–Py nanotubes can carry styrene, probably with a hydrophobic moiety.

Radical polymerization is carried out at 10°C by the addition of 5 wt% of Irgacure 369 as a photo-radical initiator; then, the decrease in the absorption of styrene is observed. It is confirmed that 90% of styrene is consumed by photoirradiation for 4 h (Supplementary Fig. 1). Figure 9c shows TEM images after polymerization. Two types of globular polymers can be found: a large one with a diameter of 20–35 nm on and/or in the membranes, and a small one with a diameter of 7–16 nm in the inner tube. These observations indicate that the resultant polymer domains are phase separated from the G–$C_2$–Py membrane during the polymerization. In this work, we cannot achieve the exact control of the polymer size; however, further investigation is expected to bring about successful results for nanosize organization through polymerization.

## Conclusions

In this study, we have shown that the dispersity of double long-chain alkylated L-glutamic acid as a molecular gelator in solvents ranging from water to *n*-hexane can be remarkably improved by ω-aminoalkylation as a simple chemical modification. This high dispersity enables the formation of highly ordered states both in aqueous and non-aqueous systems. In addition, the obtained molecular gels exhibit unique chiroptical properties based on highly ordered structures through interamide interactions. We have also demonstrated that these chiroptical properties can be controlled thermotropically and lyotropically; the chiral assemblies provide specific binding sites for achiral cyanine dye and then induce chirality for the bonded dyes. Further, we have discussed the applicability of amphiphiles to template polymerization.

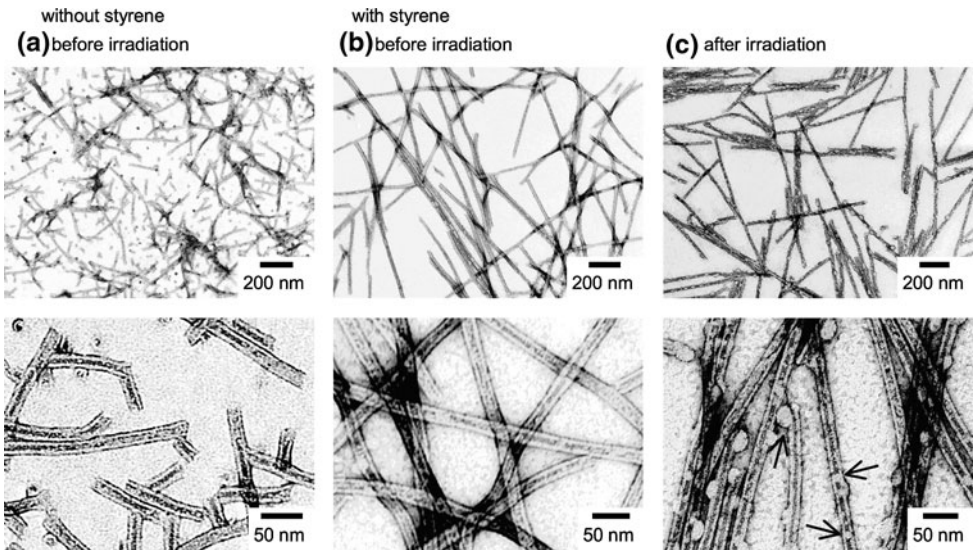


**Fig. 9** TEM images of G–$C_2$–Py (0.5 mM) without (**a**) and with styrene (0.35 mg/ml) mixture before (**b**) and after (**c**) UV irradiation (4 h) in water–methanol mixture (250:1) at 10°C

**Acknowledgments** This work was supported by the Grant-in-Aid for Scientific Research from the Ministry of Education, Culture, Sports, Science and Technology of Japan and Grant-in-Aid for JSPS Fellows from Japan Society for the Promotion of Science.

## References

Artal MC, Ros MB, Serrano JL (2001) Antiferroelectric liquid-crystal gels. Chem Mater 13:2056–2067

Becerra F, Soltero JFA, Puig JE, Schulz PC, Esquena J, Solans C (2004) Free-radical polymerization of styrene in worm-like micelles. Colloid Polym Sci 282:103–109

da Silva Gomes JFP, Sonnen AF-P, Kronenberger A, Fritz J, Coelho MAN, Fournier D, Fournier-Nöel C, Mauzac M, Winterhalter M (2006) Stable polymethacrylate nanocapsules from ultraviolet light-induced template radical polymerization of unilamellar liposomes. Langmuir 22:7755–7759

Dergunov SA, Pinkhassik E (2008) Functionalization of imprinted nanopores in nanometer-thin organic materials. Angew Chem Int Ed 47:8264–8267

Estroff LA, Hamilton AD (2004) Water gelation by small organic molecules. Chem Rev 104:1201–1218

Gopal V, Prasad TK, Rao NM, Takafuji M, Rahman MM, Ihara H (2006) Synthetic and in vitro evaluation of glutamide-containing cationic lipids for gene delivery. Bioconjug Chem 17:1530–1536

Hatano M, Yoneyama M, Sato Y, Kawamura Y (1973) Induced optical activity in poly-L-lysine-methyl orange system. Biopolymers 12:2423–2430

Hembury GA, Borovkov VV, Inoue Y (2008) Chirality-sensing supramolecular systems. Chem Rev 108:1–73

Hotz J, Meier W (1998) Vesicle-templated polymer hollow spheres. Langmuir 14:1031–1036

Ihara H, Sakurai T, Yamada T, Hashimoto T, Takafuji M, Sagawa T, Hachisako H (2002) Chirality control of self-assembling organogels from a lipophilic L-glutamide derivative with metal chlorides. Langmuir 18:7120–7123

Ihara H, Takafuji M, Sakurai T (2004) Self-assembled nanofibers. In: Nalwa HS (ed) Encyclopedia of nanoscience and nanotechnology, vol 9. American Scientific Publishers, California, pp 473–495

Kim DH, Needham D (2002) Lipid bilayers and monolayers: characterization using micropipette manipulation techniques. In: Hubbard AT (ed) Encyclopedia of surface and colloid science, vol 3. Marcel Dekker Inc., New York, pp 3057–3086

Matsui H, Kaneshima S (2002) Molecular interactions between local anesthetics and model biomembranes. In: Hubbard AT (ed) Encyclopedia of surface and colloid science, vol 3. Marcel Dekker Inc., New York, pp 3517–3534

Mishra A, Behera RK, Behera PK, Mishra BK, Behera GB (2000) Cyanines during the 1990s: a review. Chem Rev 100:1973–2012

Nakashima N, Fukushima H, Kunitake T (1981) Large induced circular dichroism of methyl orange bound to chiral bilayer membranes: its extreme sensitivity to the phase transition and the chemical structure of the membrane. Chem Lett 10:1207–1210

Oda R (2006) Molecular Gels. In: Weiss RG, Terech P (eds) Materials with self-assembled fibrillar networks. Springer, Berlin, pp 577–612

Sagawa T, Tobata H, Ihara H (2004) Exciton interactions in cyanine dye–hyaluronic acid (HA) complex: reversible and biphasic molecular switching of chromophores induced by random coil-to-double-helix phase transition of HA. Chem Commun 814–815

Shibata M, Ihara H, Hirayama C (1993) Unique property of cyanine dyes on charged poly(L-lysine). Polymer 34:1106–1108

Shimizu T, Masuda M, Minamikawa H (2005) Supramolecular nanotube architectures based on amphiphilic molecules. Chem Rev 105:1401–1444

Simalou O, Zhao X, Lu R, Xue P, Yang X, Zhang X (2009) Strategy to control the chromism and fluorescence emission of a perylene dye in composite organogel phases. Langmuir 25:11255–11260

Simonyi M, Bikádi Z, Zsila F, Deli J (2003) Supramolecular exciton chirality of carotenoid aggregates. Chirality 15:680–698

Tekobo S, Pinkhassik E (2009) Directed covalent assembly of rigid organic nanodisks using self-assembled temporary scaffolds. Chem Commun 1112–1114

Terech P, Weiss RG (1997) Low molecular mass gelators of organic liquids and the properties of their gels. Chem Rev 97:3133–3160

Timpe HJ, Ulrich S, Decker C, Fouassier JP (1993) Photoinitiated polymerization of acrylates and methacrylates with decahydroacridine-1, 8-dione/onium salt initiator systems. Macromolecules 26:4560–4566

van Esch JH, Feringa BL (2000) New functional materials based on self-assembling organogels: from serendipity towards design. Angew Chem Int Ed 39:2263–2266

Xue P, Lu R, Huang Y, Jin M, Tan C, Bao C, Wang Z, Zhao Y (2004) Novel pearl-necklace porous CDS nanofiber templated by Organogel. Langmuir 20:6470–6475